

Mechanism of Graphene Oxide Formation

Ayrat M. Dimiev^{†,‡,*} and James M. Tour^{†,‡,§,⊥,*}

[†]Departments of Chemistry, [‡]Materials Science and NanoEngineering, and [§]Computer Science, and the [⊥]Smalley Institute for Nanoscale Science and Technology, Rice University, MS-222, 6100 Main Street, Houston, Texas 77005, United States and [‡]AZ Electronic Materials, 70 Meister Avenue, Somerville, New Jersey 08876, United States

ABSTRACT Despite intensive research, the mechanism of graphene oxide (GO) formation remains unclear. The role of interfacial interactions between solid graphite and the liquid reaction medium, and transport of the oxidizing agent into the graphite, has not been well-addressed. In this work, we show that formation of GO from graphite constitutes three distinct independent steps. The reaction can be stopped at each step, and the corresponding intermediate products can be isolated, characterized, and stored under appropriate conditions. The first step is conversion of graphite into a stage-1 graphite intercalation compound (GIC). The second step is conversion of the stage-1 GIC into oxidized graphite, which we define as pristine graphite oxide (PGO). This step involves diffusion of the oxidizing agent into the preoccupied graphite galleries. This rate-determining step makes the entire process diffusive-controlled. The third step is conversion of PGO into conventional GO after exposure to water, which involves hydrolysis of covalent sulfates and loss of all interlayer registry.



KEYWORDS: graphene oxide · graphite · graphite intercalation compound

Graphene oxide (GO) is a two-dimensional material derived from graphene by introducing covalent C—O bonds.¹ The bulk form of GO, conventionally named graphite oxide, has attracted recurring interest since it was first synthesized by Brodie in 1855.² A heightened interest in GO was sparked by the upsurge of graphene-related research in 2004. Due to its ability to remain exfoliated in water as single atomic layers sheets, cast as films, and be further reduced back to graphene, GO has been successfully tested in numerous applications in electronics, conductive films, electrode materials, and composites.^{1,3,4}

Upon dissolution in water and in some organic solvents,^{5,6} bulk graphite oxide spontaneously exfoliates to single layer GO sheets. From this perspective, bulk graphite oxide can be viewed as an accumulation of GO sheets. In this work, we will use the term "GO" to signify single atomic layer sheets. We use the term conventional graphite oxide (CGO) to signify bulk graphite oxide obtained by typical oxidation and purification protocols.^{7,8} We use additional terms to

signify newly discovered forms of bulk graphite oxide.

Despite recent progress in understanding GO chemistry and structure, the mechanism of its formation gained less attention and it remains elusive. Most reported studies in this field are theoretical,^{9–11} focused on the act of introducing oxygen atoms into the graphene lattice with formation of C—O covalent bonds. These studies consider both graphene and an oxidizing agent as free-standing species with no interaction with their surroundings. However, in actuality, GO is produced from bulk graphite, where individual graphene layers are closely aligned and stacked. To attack graphene layers, the oxidizing agent needs to first penetrate between those layers.

The study here uses the modified Hummers' method of GO preparation^{7,8} that is currently the most commonly used approach. In the original Hummers' method, 3 wt equiv of potassium permanganate ($KMnO_4$) and 0.5 wt equiv of sodium nitrate were used to convert 1 wt equiv of graphite to graphite oxide. The reaction was carried

* Address correspondence to
tour@rice.edu,
ayrat.dimiev@azem.com.

Received for review January 29, 2014
and accepted February 25, 2014.

Published online February 25, 2014
10.1021/nn500606a

© 2014 American Chemical Society

out in concentrated H_2SO_4 . In the modified method, 5 wt equiv of $KMnO_4$ (with no sodium nitrate) is used, which is added sequentially after complete consumption of the previously added portion. In this work, we investigate intermediate products obtained with the use of 1, 2, 3, and 4 wt equiv of $KMnO_4$. In contrast to previous studies investigating progressively oxidized CGO samples,^{12–15} we do not analyze the final graphite oxide products obtained after their washing and drying since that gives minimal information concerning the reaction mechanism. Instead, we focus on intermediate reaction products without destroying their unique interlayer morphology by exposing them to water. Furthermore, instead of analyzing bulk quantities,^{12–15} the microscale is focused upon, employing direct real-time monitoring, a method that has been developed for studying stage transitions in graphite intercalation compounds (GICs).^{16,17}

RESULTS AND DISCUSSION

In the course of conversion of bulk graphite to GO, three independent steps can be identified. The first step is conversion of graphite to the sulfuric acid–graphite intercalation compound (H_2SO_4 –GIC), which can be considered as the first intermediate. The second step is conversion of the GIC into the oxidized form of graphite, which we define as “pristine graphite oxide” (PGO), constituting the second intermediate. The third step is conversion of PGO to GO by the reaction of PGO with water.

The first step, H_2SO_4 –GIC formation, begins immediately upon exposing graphite to the acidic oxidizing medium. The GIC formation is manifested by the characteristic deep-blue color acquired by graphite flakes. Despite the obvious simplicity of this observation, this fact was largely neglected in the modern GO-related literature, and was never systematically described in connection to the mechanism of GO formation. In addition to visual observations, the GIC formation can be confirmed by Raman spectroscopy and X-ray diffraction (XRD).^{14–16} As will be demonstrated below, the characteristics of the GIC intermediate formed in the course of GO production are identical to those of H_2SO_4 –GICs produced electrochemically or chemically.^{17–20} The rate of the H_2SO_4 –GIC formation depends on the electrochemical potential of the surrounding medium.¹⁶ Under the experimental conditions of the modified Hummers' method with flake graphite, the stage-1 GIC forms within 3–5 min. The second step, conversion of the GIC into PGO, is significantly slower; it takes several hours and even days depending on the graphite source. Thus, the stage-1 GIC can be considered as an intermediate, which can be isolated and characterized. The second step, conversion of the stage-1 GIC into PGO, is the most intriguing step.

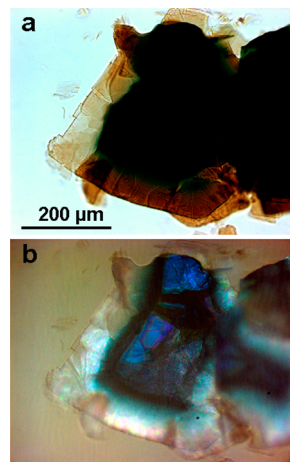


Figure 1. Optical microphotographs of a graphite flake in the course of its conversion from stage-1 H_2SO_4 –GIC to PGO: (a) transmitted light, (b) reflected light. The recorded oxidation level was achieved by addition and complete consumption of 1 wt equiv of $KMnO_4$ to the corresponding amount of graphite flakes.

Figure 1 shows a partially oxidized graphite flake in the midst of its transformation from a GIC to PGO. The recorded oxidation degree was achieved by addition of 1 wt equiv of $KMnO_4$ to the corresponding amount of graphite flakes. The micrographs were taken after complete consumption of 1 wt equiv of $KMnO_4$, which was detected by disappearance of the characteristic green color of $KMnO_4$ in H_2SO_4 . The micrographs demonstrate front-like edge-to-center progression of the chemical reaction.

Oxidized areas along the flake's perimeter appear semitransparent light-brown in transmitted light (Figure 1a) and light-yellow-pearl in reflected light (Figure 1b). The unoxidized areas in the center of the flake appear dark in transmitted light and blue-colored in reflected light. The chemical nature of the differently colored areas can be confirmed by Raman spectroscopy (Figure 2).

The Raman spectrum from the blue-colored area in the center of the flake (Figure 2a,b) contains a single feature: the G-peak at 1635 cm^{-1} . The G-band is blue-shifted due to charging of graphene layers by intercalant, and it is strongly enhanced. The enhancement is caused by elimination of destructive interference at laser energies in the vicinity of the double Fermi energy, and by increasing of the probing depth induced by intercalation.^{16,21} The 2D-band is most likely suppressed by the “Pauli blocking” effect.^{16,22} This spectrum (Figure 2b) is identical to that of the stage-1 H_2SO_4 –GIC.^{16,17} The Raman spectrum from the light-yellow-pearl-colored area along the flake perimeter (Figure 2c) contains the two broad G and D peaks and the two low intensity 2D and D + G bands. This spectrum is typical for GO.^{23,24} The spectrum acquired from the dark-looking bordering area between the blue and yellow areas (Figure 2c) is simply the sum of

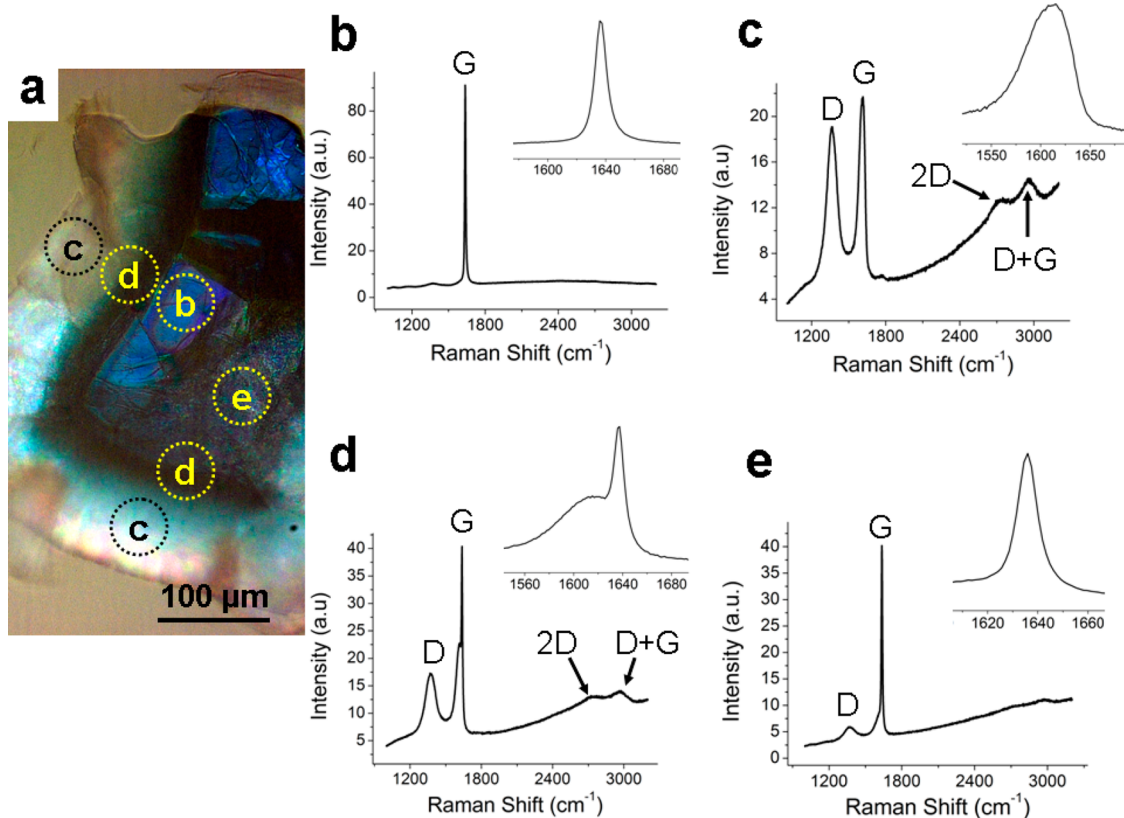


Figure 2. Raman spectra acquired from certain areas of a partially oxidized graphite flake. (a) Map of the flake showing spots of acquisition; the circles labeled “b”, “c”, “d”, and “e” indicate the four typical areas on the flake surface where the spectra were acquired. (b–e) The typical Raman spectra acquired from the corresponding spots labeled in (a). The insets represent the X-axis expansion in the G-band area. A 514 nm laser was used for excitation.

the two spectra discussed above. Thus, on the border there is a mixture of the two phases: stage-1 GIC and GO. No traces of stage-2 GIC, higher stages, or pure graphite are ever detected in our experiments. Here we arrive at our first conclusion: PGO is formed directly from the stage-1 GIC without any additional rearrangements in the graphite structure.

Upon closer inspection, the dark flake's center is not uniform. In addition to the uniformly blue-colored area (b) (Figure 2a), there is a grayish-looking area labeled with letter (e). This area appears patchy, *i.e.*, it consists of submicrometer-sized rainbow-colored patches with a dominance of blue and grayish-blue colors. The Raman spectrum acquired from this area (Figure 2e) is almost the same as the one from the uniformly blue-colored area. The presence of the low intensity D-band is the only difference. This patchy area is uniform in terms of its Raman spectrum; there is only slight variation in the D-band intensity, *i.e.*, D/G ratio. The Raman spectra taken from the oxidized edge, neighboring patchy area (spots (c) and (d)) down to the patchy area (e) on the Figure 2a) are identical to those taken from the edge neighboring the uniformly blue area (spots (c) and (d)) to the left from the uniformly blue area (b) on the Figure 2a). Flakes in the same reaction mixture are different. Along with the flakes

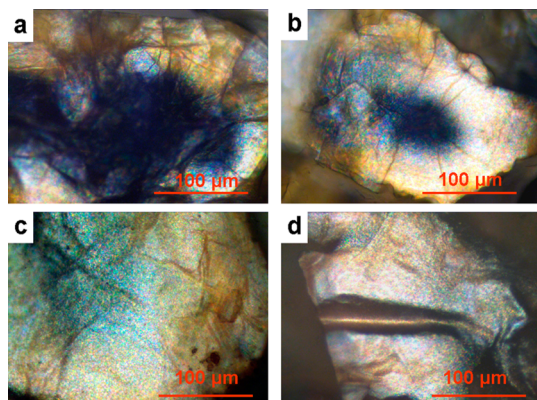


Figure 3. Optical microphotograph of graphite flakes sampled from the reaction mixture after consumption of 2 wt equiv of KMnO₄; (a and b) partially oxidized flakes; (c) almost fully oxidized flake; (d) fully oxidized flake.

comprising half-uniform-blue, half-patchy centers as seen in the Figure 1b, the reaction mixture contains flakes with only uniform-blue centers and with only patchy centers.

After consumption of the second wt equiv of KMnO₄, the size of the dark-blue center was decreased and the width of the yellow-colored GO band on the flake's edge was increased (Figure 3). Very few flakes

containing uniformly blue-colored areas were observed in the reaction mixture. Most of the flakes had patchy centers. The Raman spectra acquired from different spots of those patchy centers were very similar between each other and to those described in Figure 2e. The GO phase was not significantly detected in patchy areas. This observation suggests that the structure of patchy areas does not progressively change with oxidation; instead, the size of the patchy areas decreases. Hence, the D-band origin in the patchy area is not caused by oxidation but by the intercalation-induced changes themselves. Earlier we reported a similar reversible D-band rise during GIC stage transitions which did not involve any permanent oxidation.¹⁷

After consumption of the third wt equiv of KMnO_4 , all of the flakes sampled from the reaction mixture appeared to be completely oxidized. No dark blue-colored areas were detected by optical microscopy. Approximately 80% of the flakes looked uniformly yellow-colored. However, 20% of the flakes appeared as the one shown in Figure 3c; the flakes' centers had a slight bluish tint. The Raman spectra acquired from the slightly bluish areas were similar to those acquired from the uniformly yellow areas, suggesting the presence of only the GO phase. The Raman spectra of GO is not very sensitive toward the density of defects when the distance between the two scattering centers is $<1.5\text{ nm}$.^{23,24} It is still possible that the bluish centers have slightly fewer functional groups. In bulk quantities, the PGO flakes obtained with the use of 3 wt equiv of KMnO_4 looked darker when compared to the flakes obtained after consumption of 4 wt equiv of KMnO_4 (Figure S1, Supporting Information). Upon exposure to water, the former dispersed and exfoliated with difficulty. Nearly 48 h of swirling with repetitive sonication was required to dissolve the sample in water. Tiny multilayered, dark-brown particles were observable with the bare eye even after 48 h of swirling. The PGO made with 4 wt equiv of KMnO_4 dissolved completely after only 15 min of swirling. This observation suggests that with the 3 wt equiv of KMnO_4 , the density of functional groups was not high enough to afford spontaneous exfoliation.

The identity of the specific oxidizing agent species attacking graphene layers is not known. Moreover, even the nature of the $\text{KMnO}_4/\text{H}_2\text{SO}_4$ solution itself has not been systematically studied. Some researchers suggest that the oxidizing agent is manganese heptoxide (Mn_2O_7).¹ Indeed, the green-colored Mn_2O_7 can be isolated from the $\text{KMnO}_4/\text{H}_2\text{SO}_4$ solution of the similar color.²⁵ It is more likely, however, that in H_2SO_4 Mn(VII) exists in the form of planar permanganyl (MnO_3^{+}) cation, which is closely associated with hydrogen sulfate (HSO_4^{-}) and sulfate (SO_4^{2-}) ions in the forms of MnO_3HSO_4 , or $(\text{MnO}_3)_2\text{SO}_4$.^{26,27} In the nearly 100% H_2SO_4 solvent, the above-mentioned compounds

exist predominantly in their nonionized forms, while in more dilute acid, ionization takes place.^{26,27}

The stoichiometry of the stage-1 H_2SO_4 -GIC can be represented by the formula $\text{C}_{(21-28)}^{+}\cdot\text{HSO}_4\cdot2.5\text{H}_2\text{SO}_4$.^{16,18} The interlayer galleries in the stage-1 H_2SO_4 -GIC are closely packed with H_2SO_4 molecules and HSO_4^{-} ions, which do not form any ordered structure.^{16,18} To diffuse between the graphene layers, the oxidizing agent needs to either replace existing intercalant molecules, or insert between them. The clear edge-to-center front-like propagation of the reaction (Figures 1 and 2a) is an indication that the rate of diffusion of the oxidizing agent into the graphite interlayer galleries is lower than the rate of the chemical reaction itself. As soon as the oxidizing agent diffuses between the graphene layers, it quickly reacts with nearby carbon atoms. In an alternative scenario, the oxidizing agent would be accumulated between the graphene layers, and the oxidized areas would form randomly all over the flake. The experimental data suggests the opposite: as we mentioned above, the patchy centers do not gradually transform into PGO. Thus, the second step of PGO formation is diffusive-controlled where the oxidant replaces the acid intercalant. This is the rate-determining step of the entire GO formation process.

The progression of reaction on different flakes from the same reaction mixture was found to be different. Thus, the flakes sampled from the reaction mixture after consumption of 2 wt equiv of KMnO_4 (Figure 3) varied from almost fully oxidized through very lightly oxidized. Sixty percent of the flakes were oxidized to the level as on the Figure 3a,b and another 40% were oxidized to the level as on the Figure 3c,d. A small number of flakes ($\sim 1\%$) were found to be almost fully blue-colored in the form of the stage-1 GIC with only trace oxidation. The difference in the reaction progress on different flakes is likely caused by the flakes' morphology. It was recently shown by Eigler and co-workers²⁸ that in the same batch of as-prepared graphite oxide, among the majority of normally oxidized GO flakes, there were a relatively small number of flakes that have been minimally damaged by oxidation. This observation can be well-understood now in terms of our findings. The difference in flake morphologies causes the difference in diffusion rates, which in turn causes the differences in the degrees of oxidation.

Being diffusive-controlled, the entire PGO formation process depends on the size of the graphite flakes. Thus, for the same source of graphite, small-size flakes are oxidized significantly faster than large flakes as seen in Figure S2 (Supporting Information). While the edge-to-center reaction propagation is the same for small and large flakes, the percentage of the entire flake body that is the unoxidized blue color is significantly less for the small flakes than for the large flakes. Concerning the different graphite sources, our

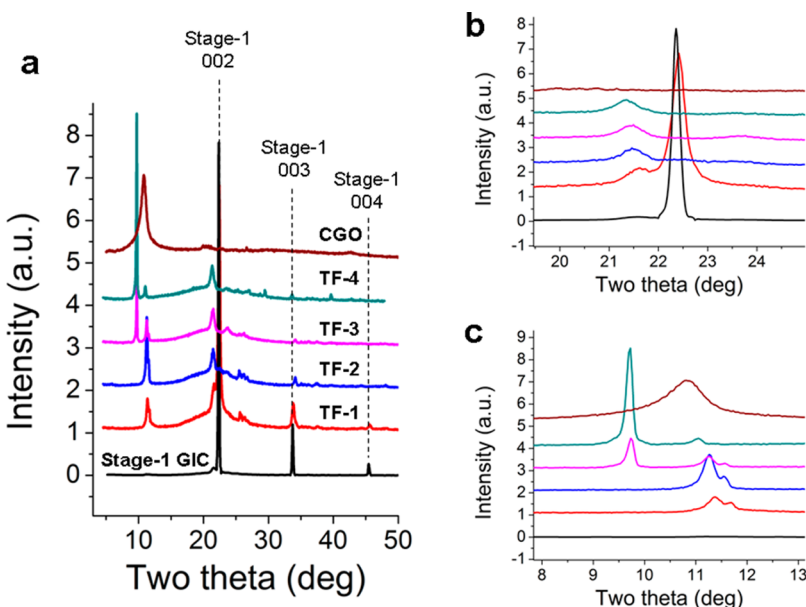


Figure 4. X-ray diffraction data. (a) X-ray diffraction patterns for stage-1 GIC (black line), CGO (brown line), and four transition forms (red, blue, pink, and dark cyan lines). The labels “TF-1” to “TF-4” represent the four consecutive transition forms obtained by consumption of 1, 2, 3, and 4 wt equiv of KMnO₄, respectively. (b and c) The X-axis expansions of (a) in the 20–24° and 8–13° 2θ diffraction angle regions.

experiments demonstrated that the time of the GIC-to-PGO conversion varied significantly depending on the mesh size and structural characteristics, which we have not yet systematically studied. As a general observation, highly crystalline graphite samples were converted to PGO significantly slower when compared to the more disordered samples. The same highly crystalline flake graphite was oxidized significantly faster if it had been subjected to thermal expansion prior to the oxidation. Thermally expanded graphite is disordered and, unlike parent graphite, does not form a continuous GIC in the C-axis direction. In addition, the change in the concentration of KMnO₄ in H₂SO₄ from 5.0 to 15.0 mg/mL did not significantly affect the rate of the reaction. Indeed, the diffusion of an oxidizing agent within two-dimensional graphite interlayer galleries should not depend on its concentration in bulk solution.

More questions remain concerning the dynamics of the oxidizing agent after it attacks graphene. Most likely, during the second step, the reduced form of the oxidizing agent remains in the interlayer galleries and is not removed (or not completely removed) until the beginning of the third step, when PGO exfoliates upon exposure to water. Thus, manganese was detected by X-ray photoelectron spectroscopy (XPS) in the PGO samples purified by some organic solvents (Figure S3), see the Supporting Information for more details. However, manganese was never detected in the water-washed and methanol-washed graphite oxide samples, where PGO completely exfoliates in corresponding solutions. This observation suggests that, unlike sulfur, manganese does not form any functionalities with long lifetimes on the GO basal planes.

The Raman data is limited by the laser spot size and the probing skin depth. To gain information concerning the broader structure of the sample, we used XRD analysis, which being performed on bulk quantities, reveals all the phases present in the specimen. In this experiment, 4 wt equiv of KMnO₄ was added sequentially to the graphite/H₂SO₄ slurry, and corresponding samples were subjected to XRD analysis after complete consumption of each weight equivalent of KMnO₄. The four samples are referred to as “transition form” (TF)-1, -2, -3, and -4, respectively. The samples were protected from moisture to prevent decomposition of their unique structure.

The graphite sample taken from the reaction mixture 20 min after addition of the first weight equivalent of KMnO₄ exhibits a diffraction pattern typical for the stage-1 H₂SO₄-GIC (Figure 4). The 002 diffraction line at 22.3° 2θ angle along with the 003 and 004 signals at 33.7 and 45.2° can be unambiguously assigned to the stage-1 H₂SO₄-GIC with the interlayer distance (d_i) of 7.98 Å.^{16,17,19,20} The stage-1 GIC is the only phase present in the sample. After the first added KMnO₄ portion is consumed (TF-1), the stage-1 GIC signals are still observable, though they are less intense. The broad curve in the 15–28° 2θ region is indicative of the formation of an amorphous phase. The new weak signals appear at 21.6, 11.4, and 11.7° 2θ diffraction angles.

After addition and consumption of the second wt equiv of KMnO₄ (TF-2), the signals associated with the stage-1 GIC are no longer present. This is consistent with the fact that the uniformly blue-colored areas were no longer observable in graphite flakes

with optical microscopy (Figure 3). Note the dark-blue patchy centers (Figure 3) which are abundant in TF-2 do not afford diffraction patterns specific for the stage-1 GIC. This is interesting because based on Raman analysis, the graphene layers are still fully intercalated with H₂SO₄. However, this fully intercalated structure is no longer orderly arranged. The three weak signals at 21.6, 11.4, and 11.7° 2θ diffraction angles become stronger. We were unable to assign these three signals to any of the known forms of graphite. They also did not match known patterns of any inorganic compounds containing potassium and/or manganese.

The new strong signal at 9.7° 2θ is observed in the sample taken after addition and consumption of the third wt equiv of KMnO₄ (TF-3). This signal becomes even stronger in TF-4. The intensity of the signals at 11.4 and 11.7° 2θ diffraction angles decreases in TF-3 and TF-4, suggesting that they do not originate from inorganic byproducts; the byproducts are accumulated with addition of more KMnO₄. The baseline in the 15–28° 2θ region flattens, indicating a decrease of the amorphous phase content. Thus, the new crystalline form of oxidized graphite, which we define as PGO, is formed.

The strong sharp signal at 9.7° 2θ diffraction angle is very different from the broad and weak 11.0° 2θ signal in CGO (Figure 4a,c). The near 11.0° 2θ signal specific for bulk CGO samples has been reported in numerous studies;^{12,13,15} however, little explanation has been provided concerning its origin. Bulk CGO is the product of restacking of previously exfoliated single layer GO flakes. It lacks any long-range ordering along the *c*-axis and, hence, should not provide a well-defined XRD pattern. The near 11.0° 2θ signal likely originates from subnm-sized ordered areas of Moiré patterns which form on rotationally faulted bilayer graphene.^{29–31} Note, GO consists of two different types of domains: intact graphene domains and oxidized domains. The two types of domains are randomly distributed throughout the GO flake.^{32,33} The oxidized domains cannot generate diffraction signals, since carbon atoms are irregularly shifted from their original positions due to sporadic formation of C–O covalent bonds. Thus, the Moiré pattern can form only by overlapping of the graphitic domains from neighboring GO flakes. This ordering has very short-range along the *c*-axis (only two neighboring GO layers), and very small integral lateral area. Thus, the 11.0° 2θ signal in CGO samples is weak. The ordered zones of the Moiré pattern gradually transform into disordered zones. The transition areas also generate diffraction at angles deviating from the main signal, thus the signal is broad.

The 9.7° 2θ signal in PGO is sharp and strong, suggesting the existence of a long-ranged highly ordered structure. Most notably, this is the structure

of the original graphite flakes subjected to a *c*-axis expansion which preserves the ordered stacking of constituent graphene layers. Sufficient and uniform oxidation of constituent graphene layers is a key requirement for building up the new crystalline PGO structure. The insufficiently oxidized TF-2 remains amorphous. The new crystalline structure starts building up in the moderately oxidized TF-3 and becomes even more crystalline in the highly oxidized TF-4. The PGO structure is relatively stable and can exist for several months with no visible change if not exposed to large amounts of water. We found that the PGO crystalline structure survives even minor dilutions with water. Figure S4 (Supporting Information) shows PGO flakes kept in 65 wt % H₂SO₄ for >3 months.

Furthermore, the diffraction signal at 9.7° 2θ originates from the intact graphitic domains of PGO flakes. The H₂SO₄ molecules must still be intercalated between the graphene layers within the graphitic domains. The interlayer distance (*d*_i) corresponding to the 9.7° 2θ diffraction angle is 9.12 Å. The 1.14 Å increase in spacing compared to the stage-1 GIC (*d*_i = 7.98 Å⁹) is likely due to insertion of oxygen atoms within the oxidized domains in addition to the existing sulfuric acid molecules. The oxidized domains with irregular structure might only be responsible for *c*-axis expansion, but not for diffraction, which can originate only from graphitic domains.

We propose two possible explanations for the observed stability of the PGO structure against its exfoliation into single layer GO. First, there is GIC-like electrostatic attraction between graphene and the intercalant within the graphitic domains. The *d*_i between the two neighboring GO flakes is increased due to the oxidized domains, but the PGO layers remain integrated due to attraction forces within the graphitic domains. To afford PGO exfoliation, the enthalpy of hydration of the resulting GO layers by water should overcome electrostatic attraction within the GIC. Hydration is driven by hydrogen bonding and by electrostatic interaction between charged GO layers and water. This results in formation of a GO in water colloid solution. In concentrated and slightly diluted H₂SO₄ the ionization of GO functional groups is suppressed, and the electrostatic charge of the GO layers is apparently not sufficient to trigger the exfoliation mechanism.

The second explanation for the PGO stability is cross-linking of two neighboring GO layers by covalent sulfates. PGO contains significant amounts of covalent sulfates as an integral part of its chemical structure.³⁴ Hydrolysis of covalent sulfates is slow, and even well-washed CGO always contains residual sulfates, which are in part responsible for the acidity of GO solutions.^{34,35} Our findings concerning covalent sulfates were recently confirmed and further developed by Eigler and co-workers who demonstrated that under

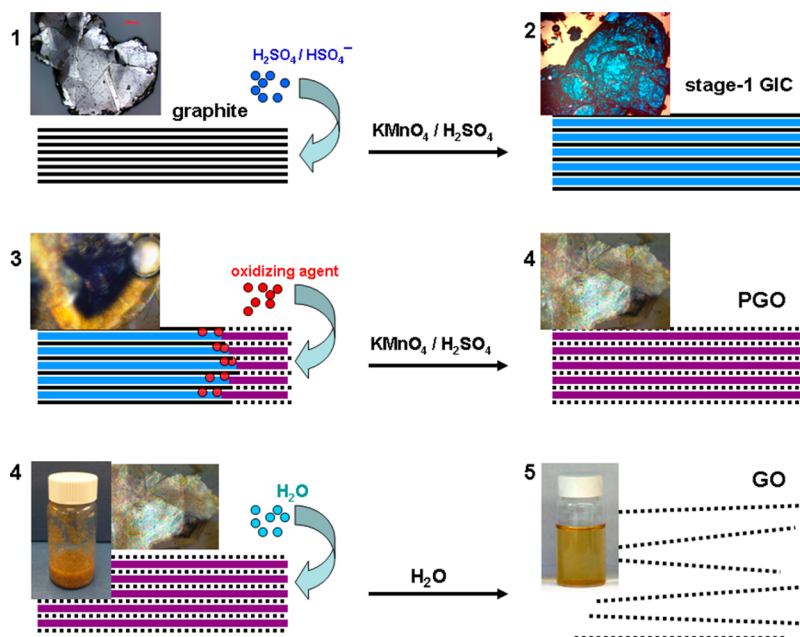


Figure 5. Schematics of conversion of bulk graphite into GO with corresponding micrographic images or sample appearances at each phase. The three steps signify formation of the two intermediate products (stage-1 GIC and PGO) and the final GO product. The solid black lines represent graphene layers; dotted black lines represent single layers of GO; wide blue lines represent $\text{H}_2\text{SO}_4/\text{HSO}_4^-$ intercalant; wide purple lines represent a layer of the mixture of $\text{H}_2\text{SO}_4/\text{HSO}_4^-$ intercalant with the reduced form of oxidizing agent.

certain conditions even CGO might contain up to 5.6 atom % sulfur.³⁶ Thus, the existence of covalent sulfates on the GO platform as a part of its chemical composition is well established. Note that H_2SO_4 molecules and HSO_4^- ions are already present in the graphite galleries when a new C–O bond forms on a graphene layer due to oxidation. Under these conditions, HSO_4^- ions and/or H_2SO_4 molecules can easily react with the newly formed epoxides immediately after they have formed, leading to covalent sulfates cross-linking two neighboring GO layers.³⁴

The third step of GO formation, conversion of PGO to GO, was investigated and discussed in previous reports.^{34,35} In addition to exfoliation into single atomic layer sheets, this step involves hydrolysis of covalent sulfates serving as protective groups, and additional modification of oxygen functionalities due to reaction

with water. Figure 5 summarizes and schematically represents the three steps constituting the process of conversion of bulk graphite into GO.

CONCLUSION

In summary, the formation of GO from bulk graphite constitutes three distinct and independent steps. The first step is conversion of graphite into a stage-1 GIC. The second step is conversion of the stage-1 GIC into an oxidized and c-axis ordered form of graphite, which we define as PGO; it involves insertion of the oxidizing agent into the preoccupied graphite galleries. This rate-determining step makes the entire process diffusive-controlled. The unique PGO structure opens greater understanding for the mechanism of GO formation. The third step is conversion of PGO into GO after exposure to water where there is no remaining c-axis order.

METHODS

Materials. The graphite flakes were obtained from Sigma-Aldrich, lots nos. 13802EH and MKBH6922V. The sulfuric acid was from Fisher Scientific, batch no. L-13345, and from J.T.Baker, batch no. 0000027217. KMnO_4 was from J.T. Baker, lot no. J41619, and from Amresco, lot no. 3413C120.

Oxidation of Graphite. Graphite flakes (400 mg, 33.3 mmol) were dispersed in 98% sulfuric acid (60 mL) at room temperature using a mechanical stirrer. After 10 min of stirring, 1 wt equiv of KMnO_4 (400 mg, 2.52 mmol) was added. The mixture became green due to the formation of the oxidizing agent MnO_3^+ . Additional portions of KMnO_4 (400 mg, 2.52 mmol each) were added when the green color of MnO_3^+ was diminished, indicating that the oxidizing agent was consumed. A total of 4 wt equiv of KMnO_4 portions were sequentially added. The end

of the oxidation was always determined by the disappearance of the green color after each KMnO_4 addition. The graphite samples of different oxidation levels were separated (see below) from the rest of the reaction mixture and used for characterization without any purification.

Monitoring the Oxidation Reaction by Optical Microscopy and Raman Spectroscopy. To acquire optical microphotographs and/or Raman spectra, the graphite flake in a certain stage of its transformation from graphite to PGO was withdrawn from the reaction mixture with a pipet and sandwiched between a microscope slide and a glass coverslip. A layer of H_2SO_4 solution was always present between the graphite surface and the coverslip; the graphite flake was free-floating in the acid mixture. Micron-sized air bubbles were occasionally floating between the coverslip and the observed graphite surface.

Samples for XRD. To acquire XRD data, the samples of graphite at different stages of oxidation were separated from the reaction mixture and separated from solution by centrifugation (30 min at 4100 rpm). The precipitated graphite samples were transferred to the XRD holder and wrapped by a polyethylene terephthalate (PET) film to shield them from atmospheric moisture. Transfer and wrapping procedures were performed under a flow of nitrogen to minimize exposure to atmospheric moisture. The wrapped samples did not show any signs of decomposition within several hours, which was confirmed by identical XRD spectra acquired within the observation time frame.

Instrumentation. Light micrographs shown in Figures 1 and 2 were acquired using a Zeiss AxioPlan 2 microscope, equipped with AxioCam MRc. The reflection mode was used with a white incandescent light source. Two types of lenses were used: Zeiss Epiplan 10 \times , 0.2 for low magnification imaging, and Zeiss LD Epiplan 20 \times , 0.4 HD DIC for higher magnification. The rest of the micrographs were acquired using a Senterra Raman microscope from Bruker equipped with an “Infinity-1” camera. The “Olympus” MPlan N 20 \times 0.40 and 50 \times 0.75 lenses were used. The Raman spectra shown in the Figure 2 were acquired using a Renishaw Raman RE01 microscope with 40 \times lens; the 514 nm wavelength laser was used for excitation. The routine Raman spectra (not shown in the manuscript) were acquired with a Senterra Raman microscope from Bruker; the 532 nm wavelength laser was used for excitation. XRD were acquired using a Rigaku D/Max 2550 diffractometer with Cu K α radiation ($\lambda = 0.15418$ nm). The data obtained were analyzed and processed using Jade 9 software package.

Conflict of Interest: The authors declare the following competing financial interest(s): Rice University has a patent filing on the modified Hummers method for GO formation. AZ Electronic Materials has licensed that intellectual property from Rice University.

Acknowledgment. This work was funded by the AFOSR (FA9550-09-1-0581), the AFOSR MURI (FA9550-12-1-0035), the ONR MURI (#00006766, N00014-09-1-1066), and AZ Electronic Materials Corp.

Supporting Information Available: Additional figures of PGO obtained with 3 and 4 wt equiv of KMnO₄; optical microphotograph of two partially oxidized flakes sampled from the same reaction mixture; the Mn2p³ XPS spectra of TFA-GO; PGO flakes after consumption of 4 wt equiv of KMnO₄. This material is available free of charge via the Internet at <http://pubs.acs.org>.

REFERENCES AND NOTES

- Dreyer, D. R.; Park, S.; Bielawski, W.; Ruoff, R. S. The Chemistry of Graphene Oxide. *Chem. Soc. Rev.* **2010**, *39*, 228–240.
- Brodie, B. Note sur un Nouveau Procédé pour la Purification et la Pesagregation du Graphite. *Ann. Chim. Phys.* **1855**, *45*, 351–353.
- Zhu, Y.; James, D. K.; Tour, J. M. New Routes to Graphene, Graphene Oxide and Their Potential Applications. *Adv. Mater.* **2012**, *24*, 4924–4955.
- Kim, J.; Cote, L. J.; Huang, J. Two Dimensional Soft Material: New Faces of Graphene Oxide. *Acc. Chem. Res.* **2012**, *45*, 1356–1364.
- Jalili, R.; Aboutalebi, S. H.; Esrafilzadeh, D.; Konstantinov, K.; Moulton, E.; Razal, J. M.; Wallace, G. G. Organic Solvent Based Graphene Oxide Liquid Crystals: A Facile Route Toward the Next Generation of Self-Assembled Layer-by-Layer Multifunctional 3D Architectures. *ACS Nano* **2013**, *7*, 3981–3990.
- Gudarzi, M. M.; Moghadam, M. H. M.; Sharif, F. Spontaneous Exfoliation of Graphite Oxide in Polar Aprotic Solvents as the Route to Produce Graphene Oxide–Organic Solvents Liquid Crystals. *Carbon* **2013**, *10.1016/j.carbon.2013.07.093*.
- Hummers, W. S.; Offeman, R. E. Preparation of Graphitic Oxide. *J. Am. Chem. Soc.* **1958**, *80*, 1339.
- Marcano, D. C.; Kosynkin, D. V.; Berlin, J. M.; Sinitskii, A.; Sun, Z.; Slesarev, A.; Alemany, L. B.; Lu, W.; Tour, J. M. Improved Synthesis of Graphene Oxide. *ACS Nano* **2010**, *4*, 4806–4814.
- Li, J.-L.; Kudin, K. N.; McAllister, M. J.; Prudhomme, R. K.; Aksay, I. A.; Car, R. Oxygen-Driven Unzipping of Graphitic Materials. *Phys. Rev. Lett.* **2006**, *96*, 176101–4.
- Sun, T.; Fabris, S. Mechanisms for Oxidative Unzipping and Cutting of Graphene. *Nano Lett.* **2012**, *12*, 17–21.
- Shao, G.; Lu, Y.; Wu, F.; Yang, C.; Zeng, F.; Wu, Q. Graphene Oxide: the Mechanism of Oxidation and Exfoliation. *J. Mater. Sci.* **2012**, *47*, 4400–4409.
- Mermoux, M.; Chabre, Y.; Rousseau, A. FTIR and ¹³C NMR Study of Graphite Oxide. *Carbon* **1991**, *29*, 469–474.
- Hontoria-Lucas, C.; Lopes-Peinado, A. J.; Lopez-Gonzalez, J. D.; Rojas-Cervantes, M. L.; Martin-Aranda, R. M. Study of Oxygen-Containing Groups in a Series of Graphite Oxides: Physical and Chemical Characterization. *Carbon* **1995**, *33*, 1585–1592.
- Szabo, T.; Berkesci, O.; Forgo, P.; Josepovits, K.; Sanakis, Y.; Petridis, D.; Dekany, I. Evolution of Surface Functional Groups in a Series of Progressively Oxidized Graphite Oxide. *Chem. Mater.* **2006**, *18*, 2740–2749.
- Krishnamoorthy, K.; Veerapandian, M.; Yun, K.; Kim, S.-J. The Chemical and Structural Analysis of Graphene Oxide with Different Degrees of Oxidation. *Carbon* **2013**, *53*, 38–49.
- Dimiev, A. M.; Bachilo, S.; Saito, R.; Tour, J. M. Reversible Formation of Ammonium Persulfate–Sulfuric Acid Graphite Intercalation Compounds and Their Peculiar Raman Spectra. *ACS Nano* **2012**, *6*, 7842–7849.
- Dimiev, A. M.; Cierotti, G.; Behabtu, N.; Zakhidov, D.; Pasquali, M.; Saito, R.; Tour, J. M. Direct, Real Time Monitoring of Stage Transitions in Graphite Intercalation Compounds. *ACS Nano* **2013**, *7*, 2773–2780.
- Eklund, P. C.; Olk, C. H.; Holler, F. G.; Spolar, J. G.; Arakawa, E. T. Raman Scattering Study of the Staging Kinetics in the C-Face Skin of Pyrolytic Graphite-H₂SO₄. *J. Mater. Res.* **1986**, *1*, 361–367.
- Yosida, Y.; Tanuma, S. In Situ Observation of X-Ray Diffraction in a Synthesis of H₂SO₄-GICS. *Synth. Met.* **1989**, *34*, 341–346.
- Inagaki, M.; Iwashita, N.; Kouno, E. Potential Change with Intercalation of Sulfuric Acid into Graphite by Chemical Oxidation. *Carbon* **1990**, *28*, 49–55.
- Chen, C.-F.; Park, C.-H.; Boudouris, B. W.; Horng, J.; Geng, B.; Girit, C.; Zettl, A.; Crommie, M. F.; Segalman, R. A.; Louie, S. G.; et al. Controlling Inelastic Light Scattering Quantum Pathways in Graphene. *Nature* **2011**, *471*, 617–620.
- Zhao, W.; Tan, H. T.; Liu, J.; Ferrari, A. C. Intercalation of Few-Layer Graphite Flakes with FeCl₃: Raman Determination of Fermi Level, Layer by Layer Decoupling, and Stability. *J. Am. Chem. Soc.* **2011**, *133*, 5941–5946.
- Kudin, K. N.; Ozbas, B.; Schniepp, H. C.; Prud'homme, R. K.; Aksay, I. A.; Car, R. Raman Spectra of Graphite Oxide and Functionalized Graphene Sheets. *Nano Lett.* **2008**, *8*, 36–41.
- Eigler, S.; Dotzer, C.; Hirsch, A. Visualization of Defect Densities in Reduced Graphene Oxide. *Carbon* **2012**, *50*, 3666–3673.
- Glemser, V. O.; Schröder, H. Zur Kenntnis des Mangan(VII)-Oxyds. *Z. Anorg. Allg. Chem.* **1953**, *271*, 293–304.
- Royer, D. J. Evidence for the Existence of the Permanganyl Ion in Sulfuric Acid Solutions of Potassium Permanganate. *J. Inorg. Nucl. Chem.* **1961**, *17*, 159–167.
- Dzhabiev, T. S.; Denisov, N. N.; Moiseev, D. N.; Shilov, A. E. Formation of Ozone during the Reduction of Potassium Permanganate in Sulfuric Acid Solutions. *Russ. J. Phys. Chem.* **2005**, *79*, 1755–1760.
- Eigler, S.; Enzelberger-Heim, M.; Grimm, S.; Hofmann, P.; Kroener, W.; Geworski, A.; Dotzer, C.; Röckert, M.; Xiao, J.; Papp, C.; Lytken, O.; Steinrück, H.-P.; Müller, P.; Hirsh, A. Wet Chemical Synthesis of Graphene. *Adv. Mater.* **2013**, *25*, 3583–35.
- Jasinski, J. B.; Dumpala, S.; Sumanasekera, G. U.; Sunkara, M. K.; Ouseph, P. J. Observation and Interpretation of

- Adjacent Moiré Patterns of Different Shapes in Bilayer Graphene. *Appl. Phys. Lett.* **2011**, *99*, 073104.
30. Ryu, G. H.; Park, H. J.; Kim, N. Y.; Lee, Z. Atomic Resolution Imaging of Rotated Bilayer Graphene Sheets Using a Low kV Aberration-Corrected Transmission Electron Microscope. *Appl. Microsc.* **2012**, *42*, 218–222.
31. Mele, E. J. Interlayer Coupling in Rotationally Faulted Multilayer Graphenes. *J. Phys. D: Appl. Phys.* **2012**, *45*, 154004.
32. Lerf, A.; He, H.; Forster, M.; Klinowski, J. Structure of Graphite Oxide Revisited. *J. Phys. Chem.* **1998**, *102*, 4477–4482.
33. Erickson, K.; Erni, R.; Zonghoon Lee, Z.; Alem, N.; Will Gannett, A.; Zettl, A. Determination of the Local Chemical Structure of Graphene Oxide and Reduced Graphene Oxide. *Adv. Mater.* **2010**, *22*, 4467–4472.
34. Dimiev, A.; Kosynkin, D. V.; Alemany, L. B.; Chaguine, P.; Tour, J. M. Pristine Graphite Oxide. *J. Am. Chem. Soc.* **2012**, *134*, 2815–2822.
35. Dimiev, A.; Alemany, L.; Tour, J. M. Graphene Oxide. Origin of Acidity and Dynamic Structural Model. *ACS Nano* **2012**, *7*, 576–588.
36. Eigler, S.; Dotzer, C.; Hof, F.; Bauer, W.; Hirsch, A. Sulfur Species in Graphene Oxide. *Chem.—Eur. J.* **2013**, *19*, 9490–9496.